MEASUREMENT OF THE MAXIMUM SPECIFIC REMOVAL RATE: UNEXPECTED INFLUENCE OF THE EXPERIMENTAL METHOD AND THE SPOT SIZE Paper M701

Conference Paper · October 2015

DOI: 10.2351/1.5063162

CITATIONS
4

READS
264

4 authors:

Benjamin Lauer
5 PUBLICATIONS **51** CITATIONS
SEE PROFILE

Beat Jaeggi
Lasea Switzerland SA
54 PUBLICATIONS **573** CITATIONS
SEE PROFILE

Yiming Zhang
Universität Bern
10 PUBLICATIONS **62** CITATIONS
SEE PROFILE

Beat Neuenschwander
Bern University of Applied Sciences
92 PUBLICATIONS **1,181** CITATIONS
SEE PROFILE

MEASUREMENT OF THE MAXIMUM SPECIFIC REMOVAL RATE: UNEXPECTED INFLUENCE OF THE EXPERIMENTAL METHOD AND THE SPOT SIZE

Paper M701

Benjamin Lauer[1], Beat Jaeggi[1], Yiming Zhang[1], Beat Neuenschwander[1]

[1] Bern University of Applied Science, Institute of Applied Laser, Photonics and Surface Technologies, Pestalozzistrasse 20, 3400 Burgdorf, Switzerland

Abstract

Ultra short laser pulses often are the tool of choice when high requirements concerning machining quality are demanded. But for industrial use the process has also to be efficient, meaning that the removal rate (ablated volume per time and average power) should be as high as possible. Many publications deal with the threshold fluence and the removal rate for various materials but often use different methods and beam parameters to determine these values. To demonstrate the influence of the different methods, the removal rate for steel and copper was determined for different pulse durations and different spot sizes using the following three different methods: With the first method the removal rate is calculated from the threshold fluence and the energy penetration depth deduced by machining craters at low repetition rates, measuring its depths and using the logarithmic ablation law. With the second method the removal rates were directly determined by measuring the volume of these craters and with the third method they were determined by measuring the volume of squares machined with a pulse overlap and higher repetition rates. This systematic study shows differences between the investigated methods themselves. Additionally it reveals for all three methods an unexpected influence of the spot size which is much more pronounced in the case of steel.

Introduction

Systems with 10 ps or shorter pulses show clear advantages concerning machining quality, heat affected zone, debris etc. [1-4]. But for industrial use the process has also to be efficient, meaning that the removal rate (ablated volume per time and average power) should be as high as possible. Many publications deal with the threshold fluence and the removal rate for various materials but often use different methods and beam parameters to determine these values.

The easiest method to determine the removal rate is to machine squares with a constant number of slices. The removal rate is calculated from the ablated volume, the processing time (laser-on-time) and the average power.

A further method to determine the removal rate from the threshold fluence and the energy penetration depth deduced by machining craters at low repetition rates, measuring its depths and using the logarithmic ablation law (depth method). The values form these experiments differ from the values calculated from the "square-method" described above.

Therefore investigations concerning the removal rate, the threshold fluence and the energy penetration depth were done for different commonly used methods. The first method is the above described depth method. With the second method the removal rates were directly determined by measuring the volume of the machined craters (crater volume method) and with the third method they were determined by measuring the volume of squares machined with a pulse overlap and high repetition rates (squares method). These investigations were done for three different spot diameters.

Theory

Ablation

For ultra short pulses the heat-transfer process in metals is described with the two temperature model [1, 6-10] where the temperatures of the electrons and the lattice are treated separately. The results of the model and the experiments show, that the ablation depth z_{abl} in the middle of the ablated crater can be written in a first approximation as a function of the peak fluence ϕ:

$$z_{abl} = \delta \cdot \ln\left(\frac{\phi}{\phi_{th}}\right) \quad (1)$$

$$\phi = \frac{2 \cdot E_p}{\pi \cdot w_0^2} \quad (2)$$

Frequently two different ablation regimes are reported [8, 11] firstly the low fluence regime where the optical penetration depth dominates and secondly the high fluence regime where the energy transport by the heat diffusion of the hot electrons dominates. In [12] it is shown that for a top hat beam the efficiency of the ablation process depends on the ratio between the threshold fluence and the applied fluence ϕ_{th}/ϕ. Similar calculations have been done for a Gaussian shaped beam as emitted by most ultra short pulsed systems [12, 14]. A general expression for the ablated volume per time of a Gaussian beam is also developed in [13, 14] and reads:

$$\dot{V} = \frac{1}{4} \cdot \pi \cdot w_0^2 \cdot \delta \cdot f \cdot \ln^2\left(\frac{\phi}{\phi_{th}}\right) \qquad (3)$$

An expression for the removal rate is obtained when equation (3) is written only in terms of applied fluence:

$$\frac{\dot{V}}{P_{av}} = \frac{1}{2}\frac{\delta}{\phi} \cdot \ln^2\left(\frac{\phi}{\phi_{th}}\right) \qquad (4)$$

All these considerations clearly show that the ablation process can be optimized. With the first derivation of (4) it is possible to calculate the threshold fluence:

$$\phi_{th} = \frac{1}{e^2}\phi_{opt} \qquad (5)$$

From the equation (5) the maximum removal rate per average power (4) then reduces to:

$$\frac{\dot{V}_{\max}}{P_{av}} = 2\frac{\delta}{\phi_{opt}} \qquad (6)$$

With (5) and (6) it is possible to calculate the threshold fluence ϕ_{th} and energy penetration depth δ when the maximum ablation rate per average power and the corresponding optimal fluence are known.

Due to incubation effects the threshold fluence also strongly depends on the number of pulses applied, which is described for metals in [12, 15-18]. Additionally it was found that also the energy penetration depth shows an incubation effect of the same kind. The maximum removal rate may therefore strongly depend on the number of pulses applied; as well. More details are given in [22, 17-19].

Calculating methods

With the depth method the removal rate is calculated from the threshold fluence and the energy penetration depth using (4). The two measurements are deduced by machining craters at low repetition rates. The measured depth is fitted with the logarithmic ablation law (1) to get the threshold fluence ϕ_{th} and energy penetration depth δ.

With the crater volume method the removal rate is calculated from the ablated volume and the number of pulses deduced by machining craters at low repetition rates. The removal rate is calculated with (7), where n is the number of pulses, E_P is the pulse energy and V the measured ablated volume.

$$\frac{\dot{V}}{P_{av}} = \frac{V}{n/f_{rep} \cdot \left(E_P \cdot f_{rep}\right)} = \frac{V}{n \cdot E_P} \qquad (7)$$

The experimental data of the removal rate as a function of the applied fluence were fitted with (4) to get the threshold fluence ϕ_{th} and energy penetration depth δ.

As these experiments are very time-consuming they are often not practicable. More time effective is the method with ablated squares where the threshold fluence ϕ_{th} and energy penetration depth δ are determined from the maximum removal rate like the crater volume method. The removal rate can be calculated by dividing the ablated volume by the machining time and the average power. The experimental data of the removal rate as a function of the applied fluence were fitted with (4) in order to get the threshold fluence ϕ_{th} and energy penetration depth δ. [20]

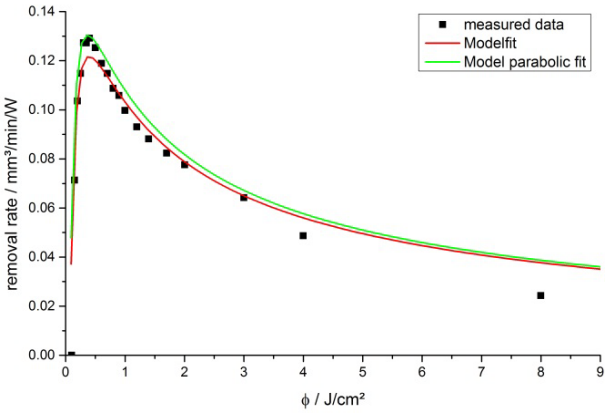

Figure 1 removal rate for stainless steel 1.4301: method with hatched squares

For the crater volume and squares method beside the least square fit of (4) to the experimental data the maximum can also be found by a parabolic fit to the data points around its peak. Out of this set of the maximal removal rate and corresponding optimal fluence a theoretical threshold fluence ϕ_{th} and energy penetration depth δ can be calculated using (5) and (6).

The comparison between the model fit and the calculated model with the values for ϕ_{th} and δ from the parabolic fit is shown in Figure 1. The parabolic fit represents the optimum very well but deviates significantly at higher fluences.

Experimental Set-Up

The radiation of the used laser source was guided via a λ/4-plate (to generate a circular polarized beam) and folding mirrors through a beam expander into a galvo scanning head where it was focused by an f-theta objective onto the target. The experiments were performed with a FUEGO™ (JDSU Ultrafast, former Time Bandwidth Products, Switzerland) ps-laser system working at a wavelength of 1064 nm with pulse duration of about 10 ps. The experiments were performed with three different spot sizes of approximately $w_0 = 15.5$ µm, 30 µm and 50 µm, respectively, different optical components were used. The focal plane was always on the sample surface. For $w_0 = 15.5$ µm and 30 µm a corresponding beam expander was used whereas for $w_0 = 50$ µm it was removed from the beam path. The beam quality factor M^2 always was better than 1.3 in all experiments. The metals used in the investigation were steel 1.4301 (AISI 301 in US) and copper Cu-DHP.

In order to deduce ϕ_{th} and δ with the depth and the crater volume method, series with single ablated craters were generated with different number of pulses for all spot sizes. We used 25, 50, 100, 250 and 500 pulses. For one series the peak fluence was raised from below up to multiples of the threshold fluence. To avoid thermal accumulation effects the repetition rate was set to 50 *Hz* with the pulse on demand option POD.

For the depth method the crater depths in the centre were deduced with a white light interferometric microscope. The two parameters ϕ_{th} and δ were then deduced by a least square fit of (1) to the experimentally obtained data. On the one side for small depth i.e. low fluences or low number of pulses the deduction of the crater depth became extensive and sometimes almost impossible. On the other side, too high fluences and pulse numbers lead to deep craters where it was no longer possible to measure the depth in the center. Therefore, the evaluable area is limited.

For the crater volume method the crater volumes were also deduced with a white light interferometric microscope. The removal rate was calculated with (7). The two parameters ϕ_{th} and δ were then deduced by a least square fit of (4) to the experimentally obtained data.

Table 1 comparison of measured and calculated values for different methods

	depth method	crater volume method	square method
ϕ_{th}	measured	calculated	calculated
δ	measured	calculated	calculated
removal rate	calculated	measured	measured

For the square method hatched squares were machined with a side length of 1 mm and a pulse-to-pulse-distance and a hatch distance of $w_0/2$. The hatch angle was turned by 10° from slice to slice. This procedure was repeated 5 times to obtain a measurable depth of the squares. The squares were machined with 200 kHz repetition rate. The depth of the ablated squares was measured with a white light interferometric microscope, as well. Further the absolute machining time was calculated from the marking speed, the side length of the square, the hatch distance, the number of slices and the number of repeats. From this the removal rate was calculated by dividing the ablated volume by the machining time and the average power. The threshold fluence and the energy penetration depth were then deduced via a least square fit as described in the previous section. For the crater volume and the square method only the removal rate is measured and the threshold fluence ϕ_{th} and the energy penetration depth δ are theoretical values. For the depth method the threshold fluence ϕ_{th} and the energy penetration depth δ are measured values and the removal rate is calculated theoretically.

Results

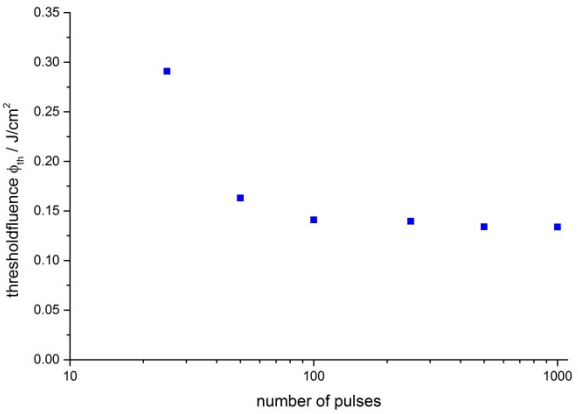

Figure 2 threshold fluence as a function of the number of pulses for steel 1.4301 and a spot radius of 49.6 µm

For the depth and the crater volume method craters with 25, 50, 100, 250 and 500 pulses were produced.

Figure 2 shows the threshold fluence as a function of the number of pulses for stainless steel 1.4301 with a spot radius w_0 = 49.6 µm. The influence of the incubation effect can clearly be seen as the threshold fluence decreases with increasing number of pulses. To avoid misinterpretations the data for 250 pulses are used for comparing the three different methods.

Depth Method

Figure 3 shows the ablated depth per pulse for copper and all three spot sizes. A quite good agreement between the measured data and the theoretical logarithmic ablation law (1) can be observed. Increasing the fluence leads to deeper craters. Surprisingly, also an influence of the spot size is visible. For w_0 = 49.6 µm and 31.45 µm the ablated depth per pulse is similar and significantly smaller than for w_0 = 15.85 µm. For the two large spot sizes and for fluences above 2 J/cm² the measured depth per pulse differs from the values expected form the logarithmic ablation law (1). This is exemplarily shown in Figure 3 for w_0 = 15.85 µm.

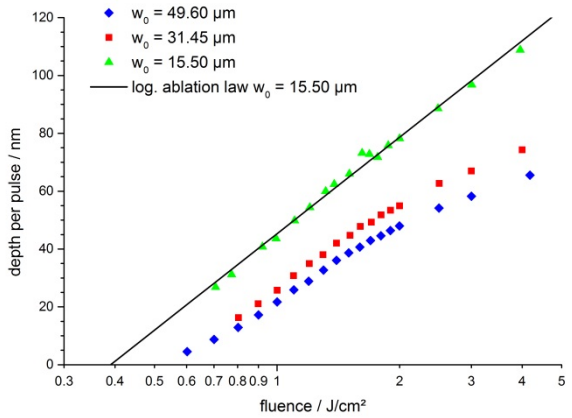

Figure 3 depth per pulse as function of the fluence for copper

Table 2 Deduced threshold fluence, penetration depths and maximum removal rate for copper

w_0 / µm	ϕ_{th} / J/cm^2	δ / nm	$\Delta V_{max}/\Delta t$ / mm^3/min/W
15.85	0.39	48.144	0.2
31.45	0.566	45.998	0.132
49.6	0.567	38.86	0.111

The differences in the ablated depth affect also the threshold fluences ϕ_{th} and penetration depths δ followed by the corresponding maximum removal rates. These values are summarized for all spot sizes in Table 2. The threshold fluence ϕ_{th} increases with increasing spot size. On the other hand the penetration depths δ decreases with increasing spot size. The w_0 = 15.85 µm the theoretically expected maximum removal rate is approximately twice as high as for w_0 = 49.6 µm.

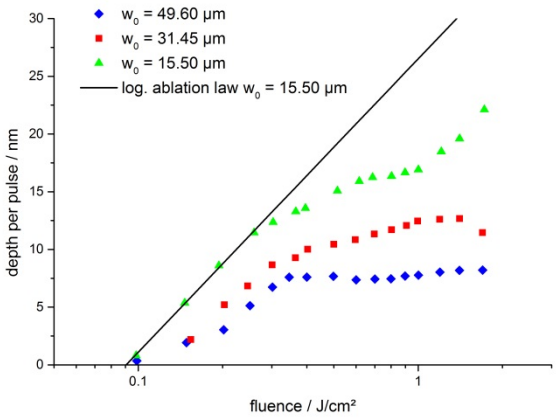

Figure 4 depth per pulse as function of the fluence for 1.4301

Figure 4 shows the ablated depth per pulse for stainless steel 1.4301 and all three spot sizes. A quite good agreement between the measured data and the theoretical logarithmic ablation law (1) only can be observed for low fluences. With w_0 = 49.6 µm it is not possible to achieve a depth per pulse of more than 8.2 nm. This is approximately the same depth as the penetration depths δ (see Table 3). With smaller spot sizes this dip is not as significant but it can still clearly be observed. For w_0 = 15.5 µm the depth per pulse starts to increase stronger for high fluences. This phenomena could not be further investigated. Due to the high aspect ratio of the holes it is not possible to measure its depth with the used microscope. In general, the depth per pulse increases with decreasing spot size.

Table 3 Deduced threshold fluence, penetration depths and maximum removal rate for 1.4301

w_0 / µm	ϕ_{th} / J/cm^2	δ / nm	$\Delta V_{max}/\Delta t$ / mm^3/min/W
15.5	0.09	11.03	0.198
31.45	0.113	8.4	0.121
49.6	0.140	8.54	0.099

This can be observed by deducing the threshold fluences ϕ_{th}, penetration depths δ and the corresponding maximum removal rates. These values are summarized for all spot sizes in Table 3. For the least square fit of (1) only the data for low fluences before the dip were used. The threshold fluence ϕ_{th} increases with increasing spot size. On the other hand the penetration depths δ decreases with increasing spot size. For w_0 = 15.85 µm the theoretical maximum removal rate is approximately twice as high as for

w_0 = 49.6 µm. Similar behavior is observed for copper, as well.

Crater Volume Method

Figure 5 and Figure 6 shows the measured removal rates and the corresponding least square fits with the model function (7) for copper and stainless steel 1.4301 for 250 pulses and w_0 = 31.35 µm. A quite good agreement between the experiment and the model can be observed. For high fluences the model differs from the measured data but this effect is stronger for steel than for copper. Similar results have been achieved for all spot sizes. Because of the sharp drop for steel 1.4301 the maximum removal rate is determined with a parabolic fit around the optimum point to deduce the maximum removal rate and the corresponding fluence. From these data the threshold fluence ϕ_{th} and the energy penetration depth δ can be determined using (8) and (9). In this investigation both methods lead to the same values. Therefore the values for the parabolic fit are not shown here.

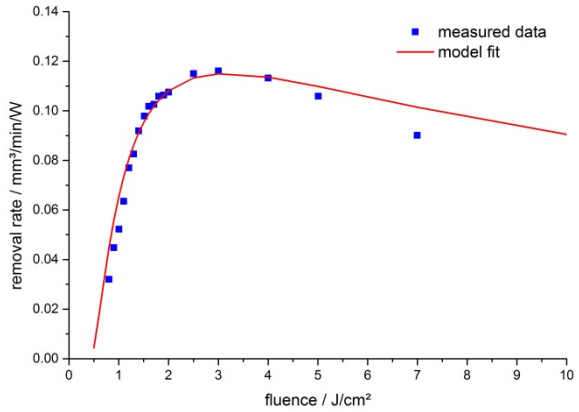

Figure 5 removal rates and the corresponding model function for copper and w_0 = 31.45 µm

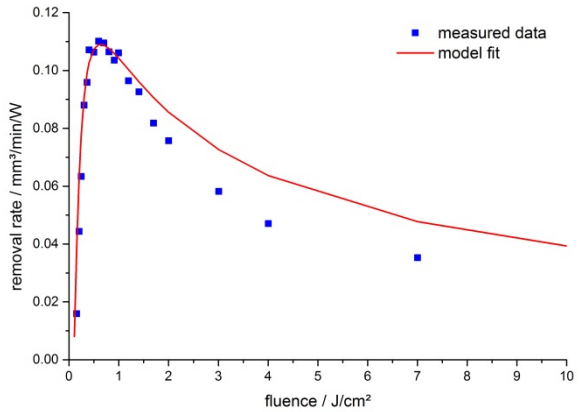

Figure 6 removal rates and the corresponding model function for 1.4301 and w_0 = 31.45 µm

The deduced threshold fluences ϕ_{th}, penetration depths δ and corresponding maximum removal rates are summarized for all spot sizes in Table 4 for copper and Table 5 for steel 1.4301.

Table 4 Deduced threshold fluence, penetration depths and maximum removal rate for copper

w_0 / µm	ϕ_{th} / J/cm^2	δ / nm	$\Delta V_{max}/\Delta t$ / mm^3/min/W
15.85	0.263	16.668	0.103
31.45	0.428	30.325	0.116
49.6	0.513	33.201	0.105

For copper the threshold fluences ϕ_{th} and penetration depths δ increases with increasing spot sizes. This leads to almost the same maximum removal rate for all three spot sizes.

Table 5 Deduced threshold fluence, penetration depths and maximum removal rate for 1.4301

w_0 / µm	ϕ_{th} / J/cm^2	δ / nm	$\Delta V_{max}/\Delta t$ / mm^3/min/W
15.85	0.071	5.13	0.118
31.45	0.086	5.74	0.109
49.6	0.096	4.74	0.08

Also for stainless steel 1.4301 the threshold fluences ϕ_{th} increase with increasing spot sizes. The penetration depths δ only differs slightly for different spot sizes. Because of this the maximum removal rate increases with decreasing spot diameter.

Square Method

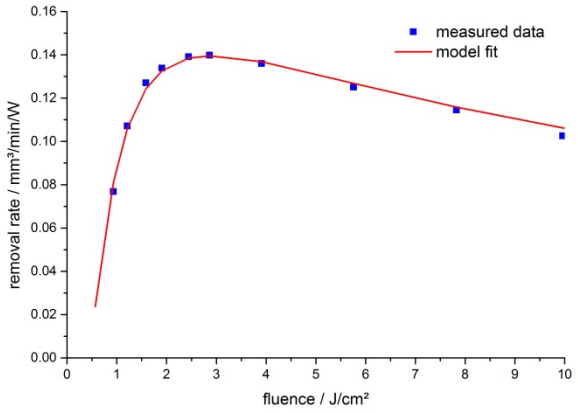

Figure 7 removal rates and the corresponding model function for copper and w_0 = 15.5 µm

Figure 7 shows the measured removal rates and the corresponding least square fits with the model function (7) exemplarily for copper for w_0 = 15.5 µm. As with the crater volume method a quite good agreement between the experiment and the model can be

observed. Also for steel a good agreement is observed even for high fluences. Therefore, there is no need to perform a parabolic fit.

The deduced threshold fluences ϕ_{th}, penetration depths δ and corresponding maximum removal rates are summarized for all spot sizes in Table 6 for copper and Table 7 for steel 1.4301.

Table 6 Deduced threshold fluence, penetration depths and maximum removal rate for copper

w_0 / µm	ϕ_{th} / J/cm^2	δ / nm	$\Delta V_{max}/\Delta t$ / mm^3/min/W
15.5	0.393	33.76	0.14
32.4	0.529	43.87	0.135
52.8	0.535	38.34	0.116

For copper the smallest spot size achieves the smallest threshold fluences ϕ_{th}. For the two larger spot sizes a significantly higher threshold fluence ϕ_{th} is calculated. The same behavior is reflected in the penetration depths δ, with $w_0 = 32.4$ µm showing the highest penetration depths δ. Therefor the maximum removal rate for $w_0 = 15.5$ µm and 32.4 µm is in the same range. Further the large spot size with $w_0 = 52.8$ µm generates a significantly lower removal rate.

Table 7 Deduced threshold fluence, penetration depths and maximum removal rate for 1.4301

w_0 / µm	ϕ_{th} / J/cm^2	δ / nm	$\Delta V_{max}/\Delta t$ / mm^3/min/W
15.5	0.06	4.8	0.13
32.4	0.078	5.89	0.123
52.8	0.092	6.15	0.109

Steel shows a behavior similar to copper. With increasing spot sizes the threshold fluences ϕ_{th} and the penetration depths δ increases. Therefor the maximum removal rate for $w_0 = 15.5$ µm and 32.4 µm is in the same range, whereas the large spot size of $w_0 = 52.8$ µm generates a significantly lower removal rate.

Comparison

First the depth method is compared with the crater volume method because both methods are based on the same craters. For a better comparison the removal rate as a function of the fluence is calculated using (7) with the deduced threshold fluences ϕ_{th} and penetration depths δ from the depth method. Figure 8 -10 show this comparison exemplarily for copper.

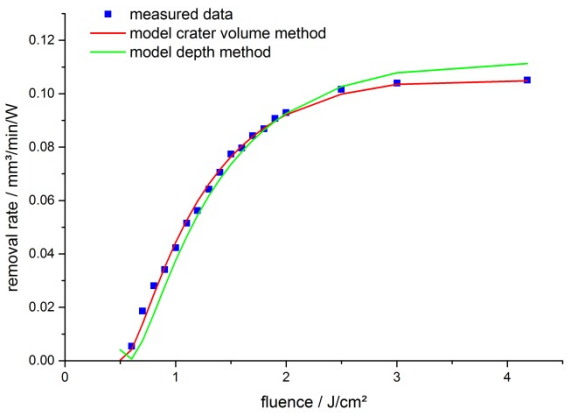

Figure 8 comparison of measured volume data, carter volume method and depth method for copper, $w_0 = 49.6$ µm and 250 pulses

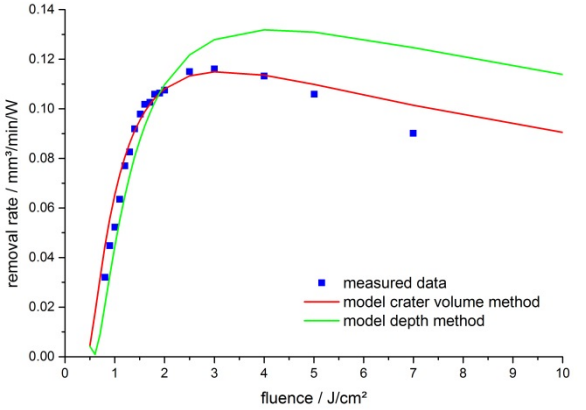

Figure 9 comparison of measured volume data, carter volume method and depth method for copper, $w_0 = 31.45$ µm and 250 pulses

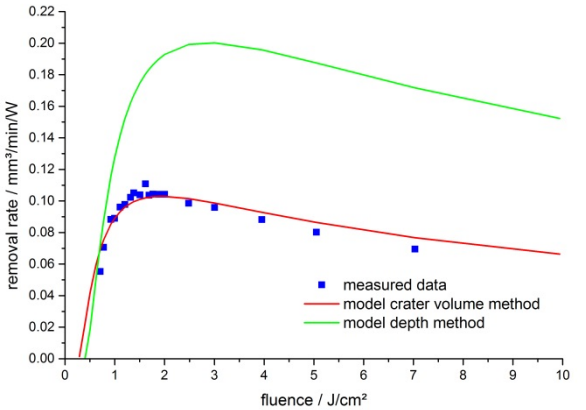

Figure 10 comparison of measured volume data, carter volume method and depth method for copper, $w_0 = 15.85$ µm and 250 pulses

Figure 8 shows a quiet good agreement between both models for $w_0 = 49.6$ µm. With decreasing spot size the difference between the two methods increase as illustrated in Figure 10 for $w_0 = 15.85$µm. The

maximum removal rate deduced by the depth method is twice as high as for the crater volume method and is only a theoretically calculated value. In this calculation it is assumed that the ablated crater is parabolic. This seems to be true for large spot sizes (here only w_0 = 49.6 µm). For smaller spot sizes the differences strongly increases and the assumption of parabolic craters seems to fail.

For stainless steel 1.4301 this difference even occurs for the largest investigated spot size. In Figure 4 it was shown that the depth per pulse for steel has a dip. For a certain fluence the depth per pulse does not further increase with increasing fluence. Figure 11 shows that in spite of constant depth the volume still continuously grows. For the depth method only the increasing part of the measured depth is used to calculate the threshold fluences ϕ_{th} and penetration depths δ. Because of that there is no good agreement between both methods. With decreasing spot size the differences increase.

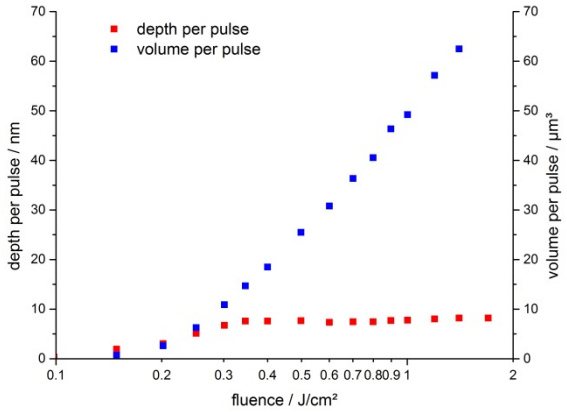

Figure 11 depth and volume per pulse as function of the fluence for 1.4301, 250 Pulses and w_0 = 49.6 µm

The increasing volume per pulse with increasing fluence by constant depth implies that for large spot sizes only a depth in the range of the penetration depths δ can be achieved. The constant depth means that the logarithmic ablation law (1) is not suitable for fluences above the optimum ablation fluence. For smaller spot sizes additionally effects provide greater depths per pulse than the penetration depths δ.

In the next part, due to the disagreement between the depth method and the measured volume only the two volume methods i.e. the crater volume and square method, are compared as illustrated in Figure 12. The square method always yields to higher removal rates than the crater volume method. Additionally the difference between the three spot sizes is smaller than for the methods using single pulse craters.

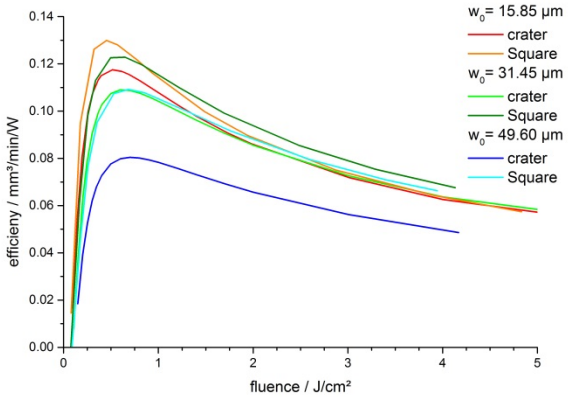

Figure 12 comparison of both volume methods, crater volume method and square method for 1.4301

Conclusion

Three different methods for the determination of the removal rate, the threshold fluence ϕ_{th} and the energy penetration depth δ were investigated. The investigations show partially huge differences between the different methods.

The depth method is good to determine the threshold fluence ϕ_{th} and energy penetration depth δ for low fluences. For high fluences the logarithmic ablation law is not suitable to calculate the depth per pulse. For steel 1.4301 and a large spot the depth per pulse stays constant beyond certain fluence and the corresponding ablated depth per pulse is in the range of the energy penetration depth δ. The theoretically calculated removal rate from the threshold fluence and the energy penetration depth is in a good agreement with the measured data only for large spot sizes whereas for smaller spot sizes the disagreement increases with decreasing spot sizes. For smaller spot sizes, it is possible to achieve depths per pulse, which are deeper than the energy penetration depth δ.

The crater volume method always shows smaller removal rates than the theoretically calculated values using the depth method. The deduced volumes as a function of the applied fluence are in good agreement with the theoretical values even when the ablated craters are not really parabolic as shown by the experiments.

Machining squares is the most application-oriented method. The removal rate is determined with a hatched square with a repetition rate of 200 kHz. These investigations show in general a higher removal rate than the crater volume method.

The investigations reveal for all three methods an unexpected influence of the spot size which is much

more pronounced in the case of steel. The removal rate decreases with increasing spot sizes. For the methods with single pulse craters a greater influence is observed than for the method with hatched squares.

Further investigations are needed to clarify the influence of the spot sizes. To check the influence of melting effects additional experiments with shorter pulse durations in the fs-regime will be done.

References

[1] B. N. Chichkov, C. Momma, S. Nolte, F. von Alvensleben and A. Tünnermann, „Femtosecond, picosecond and nanosecond laser ablation of solids“, Appl. Phys. A 63, 109 (1996).

[2] Detlef Breitling, Andreas Ruf and Friedrich Dausinger, “Fundamental aspects in machining of metals with short and ulrashort laser pulses”, Proc. SPIE 5339, 49-63 (2004)

[3] Friedrich Dausinger, Helmut Hügel and Vitali Konov, “Micro-machining with ultrashort laser pulses: From basic understanding to technical applications”, Proc. SPIE Vol. 5147, 106-115 (2003)

[4] J. Meijer, K. Du, A. Gillner, D. Hoffmann, V. S. Kovalenko, T. Masuzawa, A. Ostendorf, R. Poprawe, W. Schulz, “Laser Machining by Short and Ultrashort Pulses – State of the Art”, Annals of the CIRP, 51/2 (2002)

[5] J. M. Liu, “Simple technique for measurements of pulsed Gaussian-beam spot sizes”, Optics Letters, Vol. 7, No. 5 (1982)

[6] C. Momma, B.N. Chichkov, S. Nolte, F. van Alvensleben, A. Tünnermann, H. Welling and B. Wellegehausen, “Short-pulse laser ablation of solid targets“, Opt. Comm. 129, 134-142 (1996)

[7] C. Momma, S. Nolte, B.N. Chichkov, F. van Alvensleben and A. Tünnermann, “Precise laser ablation with ultrashort pulses“, Appl. Surf. Science 109/110, 15-19 (1997)

[8] S. Nolte, C. Momma, H. Jacobs, A. Tünnermann, B.N. Chichkov, B. Wellegehausen and H. Welling, “Ablation of metals by ultrashort laser pulses”, J. Opt. Soc. Am. B, Vol. 14, No. 10 (1997)

[9] S.I. Anisimov and B. Rethfeld, “On the theory of ultrashort laser pulse interaction with a metal”, Proc. SPIE 3093, 192-203 (1997)

[10] B.H. Christensen, K. Vestentfort and P. Balling, “Short-pulse ablation rates and the two-temperature model”, Appl. Surf. Science 253, 6347-6352 (2007)

[11] P. Mannion, J. Magee. E. Coyne and G.M. O’Conner, “Ablation Thresholds in ultrafast laser micro-machining of common metals in air”, Proc. of SPIE vol. 4876, 470-478 (2002)

[12] B. Neuenschwander et al., “Optimization of the volume ablation rate for metals at different laser pulse-durations from ps to fs”, Proc. of SPIE vol. 8243, 824307-1 (2012)

[13] B. Neuenschwander, G. Bucher, C. Nussbaum, B. Joss, M. Muralt, U. Hunziker et al., "Processing of dielectric materials and metals with ps-laserpulses: results, strategies limitations and needs", Proceedings of SPIE vol. 7584, (2010)

[14] G. Raciukaitis, M. Brikas, P. Gecys, B. Voisiat, M. Gedvilas, "Use of High Repetition Rate and High Power Lasers in Microfabrication: How to keep Efficiency High?", JLMN Journal of Laser Micro/Nanoengineering, Vol. 4 (3), 186-191 (2009)

[15] Y. Jee, M.F. Becker and R.M. Walser, “Laser-induced damage on single-crystal metal surfaces”, J. Opt. Soc. Am. B5, (1988)

[16] P.T. Mannion, J. Magee, E. Coyne, G.M. O’Connor and T.J. Glynn, “The effect of damage accumulation behavior on ablation thresholds and damage morphology in ultrafast laser micro-machining of common metals in air”, Appl. Surface Science 233, 275 – 287 (2004)

[17] M. Schmid, B. Neuenschwander, V. Romano, B. Jaeggi and U. Hunziker, "Processing of metals with ps-laser pulses in the range between 10ps and 100ps", Proc. of SPIE Vol. 7920, paper 792009 (2011)

[18] B. Jaeggi, B. Neuenschwander, M. Schmid, M. Muralt, J. Zuercher and U. Hunziker, "Influence of the Pulse Duration in the ps-Regime on the Ablation Efficiency of Metals", Physics Procedia 12, 164-171 (2011)

[19] B. Neuenschwander, B. Jaeggi, M. Schmid, U. Hunziker, B. Luescher, C. Nocera, "Processing of industrially relevant non metals with laser pulses in the range between 10 ps and 50 ps", ICALEO 2011, Paper M103 (2011)

[20] B. Lauer, B. Neuenschwander, B. Jaeggi, M. Schmid, „From fs – ns: Iinfluence of the pulse duration

onto the material removalrate and machining quality for mateals". ", ICALEO 2013, Paper M309 (2013)

Meet the author

Benjamin Lauer has a Diplom Physik (advanced degree in physics) from TU Kaiserslautern, Germany. During his studies he specialized in laser systems and laser material processing. He gained his first practical experience in the field of laser cutting and welding in industry. Now he is PhD-student at the Bern University of Applied Science. He is currently a research fellow at the Institute for Applied Laser, Photonics & Surface Technologies, investigating laser micro processing.